



HAL
open science

Numerical evidence of universal scaling for the scalar variance spectrum in forced homogeneous turbulence

Jean-Baptiste Lagaert, Guillaume Balarac, Georges-Henri Cottet

► **To cite this version:**

Jean-Baptiste Lagaert, Guillaume Balarac, Georges-Henri Cottet. Numerical evidence of universal scaling for the scalar variance spectrum in forced homogeneous turbulence. 2012. hal-00769144v1

HAL Id: hal-00769144

<https://hal.science/hal-00769144v1>

Preprint submitted on 28 Dec 2012 (v1), last revised 2 Mar 2013 (v2)

HAL is a multi-disciplinary open access archive for the deposit and dissemination of scientific research documents, whether they are published or not. The documents may come from teaching and research institutions in France or abroad, or from public or private research centers.

L'archive ouverte pluridisciplinaire **HAL**, est destinée au dépôt et à la diffusion de documents scientifiques de niveau recherche, publiés ou non, émanant des établissements d'enseignement et de recherche français ou étrangers, des laboratoires publics ou privés.

Numerical evidence of universal scaling for the scalar variance spectrum in forced homogeneous turbulence

J.-B. Lagaert^{1,2}, G. Balarac¹ and G.-H. Cottet²

¹ Grenoble-INP / CNRS / UJF-Grenoble 1, LEGI UMR 5519, Grenoble, F-38041, France

² Grenoble-INP / CNRS / UJF-Grenoble 1, LJK UMR 5224, Grenoble, F-38041, France

(Dated: December 18, 2012)

Abstract

In this letter, the spectrum of high Schmidt number passive scalar in forced homogeneous isotropic turbulence is studied through direct numerical simulations. An hybrid spectral-particle method¹ is used with a finer resolution of the scalar than of the momentum and large time-steps. This approach enables to perform a systematic analysis over a wide range of Schmidt numbers. Our results recover the theoretical scaling for the variance scalar spectrum, and its relationship with the value of the Schmidt number, for large, intermediate and small scales. The influence of the form of the scalar forcing is also discussed.

The prediction of the dynamics of a scalar advected by a turbulent flow is an important challenge in many applications. The scalar field can be used to describe the temperature field or the concentration of chemical species, for example. For a passive scalar, Z , the transport equation is an advection-diffusion equation,

$$\frac{\partial Z}{\partial t} + \vec{u} \cdot \vec{\nabla} Z = \vec{\nabla} \cdot (\kappa \vec{\nabla} Z) \quad (1)$$

where κ is the molecular scalar diffusivity and \vec{u} the turbulent velocity field. Similar to the Kolmogorov scale, η_K , which describes the smallest scale of turbulence motions beyond which dissipation dominates, the Batchelor scale, η_B , describes the smallest length scale of the scalar fluctuations that can exist before being dominated by molecular diffusion. The phenomenology of passive scalar diffusion depends on the molecular Schmidt numbers, the viscosity-to-diffusivity ratio, $Sc = \nu/\kappa$. For high Schmidt number, the Batchelor scale is smaller than the Kolmogorov scale. This means that scalar dynamics can occur at scales smaller than the smallest eddy. An important theoretical result is the influence of the Schmidt number on the scalar variance spectrum behavior². For a Schmidt number larger than one, Batchelor³ explained that the classical Corrsin-Obukhov cascade associated with a $k^{-5/3}$ law (where k is the wave number) for the scalar variance spectrum^{4,5} is followed by a viscous-convective range with a k^{-1} power law. This viscous-convective range is followed by the dissipation range, where various theoretical scalings have been proposed for the spectrum^{3,6}. However some recent numerical results⁷ seem to indicate that the $k^{-5/3}$ law appears only for very high Reynolds numbers and that the k^{-1} law exists even for Schmidt numbers smaller than one. These results were obtained by using a uniform mean scalar gradient to maintain scalar variance⁸.

For DNS of scalar mixing at high Schmidt number, the dependence of the Batchelor scale on the Schmidt number suggests that the prediction of scalar dynamics for high Schmidt numbers is more demanding in terms of spatial resolution than the prediction of momentum. In Cottet et al⁹, an hybrid particle-grid method with different grid resolutions, using particles of vorticity and scalar advected in a flow recovered through a spectral solver, was proposed. In Lagaert et al.¹, this method was extended to couple a full spectral Navier-Stokes solver with a fourth order particle method¹⁰ for the scalar. This method was used to investigate scalar transport for a wide range of Schmidt numbers. An interesting feature of this method, due to the lagrangian nature of the particle method, is that refining the scalar resolution

R_λ	N^u	$\eta_K/\Delta x^u$	Δt^u	Sc	N^z	$\eta_B/\Delta x^z$	Δt^z	Δt_{spec}^z
130	256	0.55	$1.2e^{-2}$	0.7	512	0.66	$4.3e^{-2}$	$6e^{-3}$
				4	1024	1.08		$3e^{-3}$
				8	1024	0.78		$3e^{-3}$
				16	1536	0.83		$2e^{-3}$
				32	1536	0.59		$2e^{-3}$
				64	2048	0.56		$1.5e^{-3}$
				128	3064	0.57		$1e^{-3}$
210	512	0.57	$3e^{-3}$	0.7	770	1.03	$1e^{-2}$	$2e^{-3}$
				4	1024	0.56		$1.5e^{-3}$

TABLE I. Setup of simulations performed. N^u , Δx^u and Δt^u are the number of points in each direction, the spatial step and the time step, respectively, used to solve the Navier-Stokes equation with a pseudo-spectral solver. N^z , Δx^z and Δt^z are the number of points in each direction, the spatial step and the time step, respectively, used to solve the scalar transport equation with the particle method. Δt_{spec}^z is the time step which would be needed if a pseudo-spectral method was used for the same number of scalar grid points.

to account for smaller scales in the scalar does not impose decreasing the time-step. This feature leads to additional computational savings compared e.g. to the hybrid spectral/finite-difference strategy of Gotoh et al.¹¹. Table I indicates the time-step values used in our different simulations. These simulations ran on 512 to 8192 cores of an IBM Blue Gene-P cluster with an excellent scalability (85% for the biggest configuration). For the biggest configuration, with 256^3 (resp 3064^3) resolution of the momentum (resp for the scalar) running on 8192 cores, the CPU time of our simulations would correspond to about 1.8 seconds per time-step if the scalar equation was solved with a CFL condition given by a spectral method. In the present paper we further exploit the computational efficiency of this method to investigate universal scalings of the scalar. We also discuss the discrepancy between our results and those obtained by using a uniform mean gradient by Donzis et al.⁷.

Based on this hybrid solver, various simulations have been performed in the context of forced homogenous isotropic turbulence (HIT), in a 3D periodic box with a length 2π .

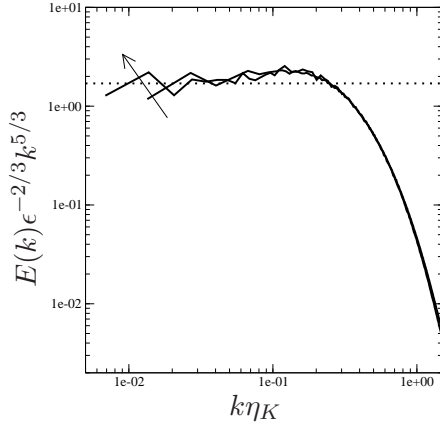


FIG. 1. Energy spectra for both Reynolds numbers, $R_\lambda \approx 130$ and $R_\lambda \approx 210$. The spectra are compensated by the Kolmogorov scaling and the dotted line is for $C_K = 1.8$. The arrow shows the direction of increasing Reynolds numbers.

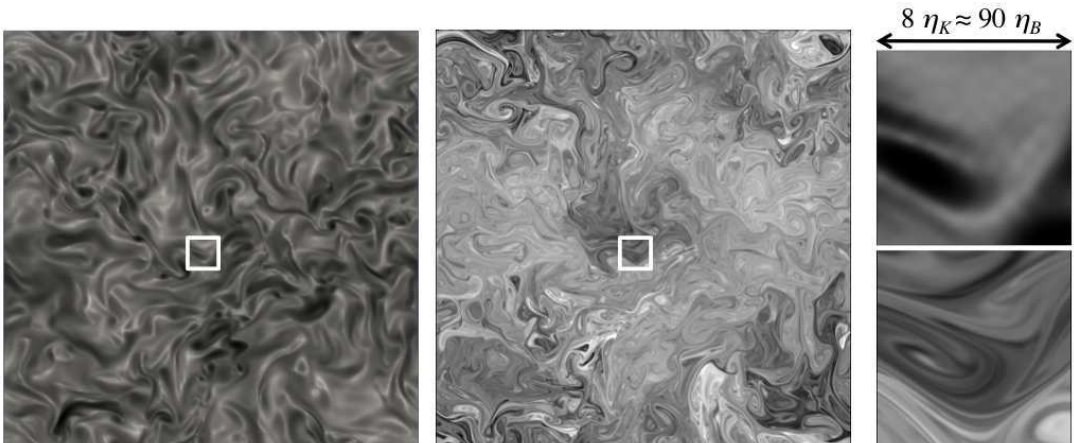


FIG. 2. $x - y$ plan colored by the vorticity magnitude (left, dark regions are for the highest vorticity values) and by the passive scalar (middle, dark regions are for the highest scalar values) for $R_\lambda \approx 130$ and $Sc = 128$. The zooms (right) correspond to the white box with a length of $8\eta_K$ for the vorticity magnitude (top) and the scalar (bottom).

The forcing scheme used to obtain a statistical steady flow follows the one proposed by Alvelius¹². To achieve a steady state for the scalar, a forcing scheme is also applied to low wave number modes in Fourier space, similarly to velocity forcing¹³. Two Taylor-scale Reynolds number, R_λ , are considered, 130 and 210, using a resolution of 256^3 and 512^3 grid

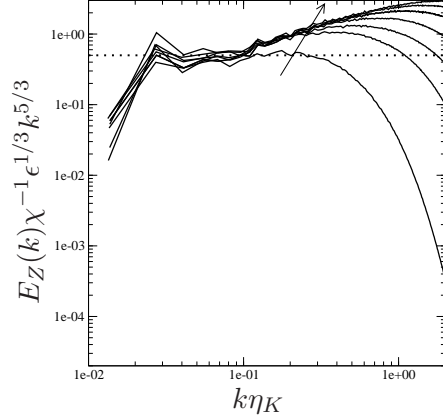


FIG. 3. Scalar variance spectra for $R_\lambda \approx 130$. The spectra are compensated by the scaling proposed by Corrsin-Obukov and the dotted line is for $C_{CO} = 0.5$. The arrow shows the direction of increasing Schmidt numbers.

points, respectively. Figure 1 shows the compensated spectrum for the kinetic energy, with ϵ , the mean energy dissipation rate. For the scalar field, the mesh resolution is increased with the Schmidt number¹⁴. Simulation details are given in table I. Figure 2 illustrates the scales separation between the Kolmogorov and Batchelor scales for the highest Schmidt number case, $Sc = 128$.

The behaviors of the scalar variance spectrum are studied at large, intermediate and small scales from this DNS database and compared with theoretical predictions. First, at the largest scales, the classical Corrsin-Obukhov cascade is expected to characterize the inertial-convective range. Similarly to the inertial range of the kinetic energy spectrum, it is expected that this cascade follows a $k^{-5/3}$ law^{4,5}. Figure 3 shows the scalar spectra for various Schmidt numbers, compensated by the Corrsin-Obukhov scaling, with χ the mean scalar dissipation rate. As expected, the results show a inertial-convective range independent of the Schmidt number. The Corrsin-Obukhov constant, C_{CO} , is found around 0.5. This result is consistent with previous results considering three-dimensional and one dimensional scalar variance spectra^{8,15}. The $k^{-5/3}$ range of the scalar spectrum is found more clearly than the $k^{-5/3}$ range of the energy spectrum. Indeed, intermittency effect can alter the value of this exponent¹⁶, but the scalar spectrum exponent is known to tend to the $-5/3$ value more rapidly than the energy spectrum exponent^{17,18}. Note that the end of the inertial-convective range appears around $10\eta_K$ (which is roughly the Taylor scale) independently of the Schmidt

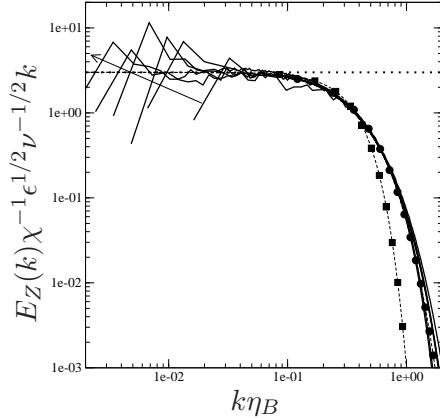


FIG. 4. Scalar variance spectra for $R_\lambda \approx 130$. The spectra are compensated by the scaling proposed by Batchelor for Schmidt number higher than one, and the dotted line is for $C_B = 3$. The arrow shows the direction of increasing Schmidt numbers. For the dissipative region, the circles show the law proposed by Kraichnan and the squares show the law proposed by Batchelor.

number.

Beyond this range, for Schmidt numbers larger than one, Batchelor³ explained the development of the viscous-convective range with a k^{-1} law. This scaling is due to the velocity small scales strain effect on the scalar field. Figure 4 shows the scalar spectra for various Schmidt numbers, compensated by the Batchelor's scaling. For the highest Schmidt number considered (128), the k^{-1} range extends to about a decade. The Batchelor constant, C_B , is found around 3. This value is in the range given in previous numerical or analytical works^{7,19,20} and larger than the theoretical value of 2 initially proposed by Batchelor. Even if all the spectra collapse at the smallest scales, in the dissipative region, the spectrum for $Sc = 0.7$ (the smallest Schmidt number value shown on the figure) has not a clear k^{-1} range. This range is found only for $Sc > 1$. The form of the scalar variance spectrum in the dissipation range (following the viscous-convective range) is also studied. Two distinct theoretical behaviors have been proposed by Batchelor³ and Kraichnan⁶, respectively. Note that this question has some practical implications for better understanding energy transfer between ocean and atmosphere²¹. Our DNS results clearly show a good agreement with the Kraichnan form, as already established in various previous works^{7,21,22}.

Compared to previous studies and observations^{8,22}, our numerical results find the same behavior for the smallest scales. However, our numerical results clearly show a $-5/3$ inertial-

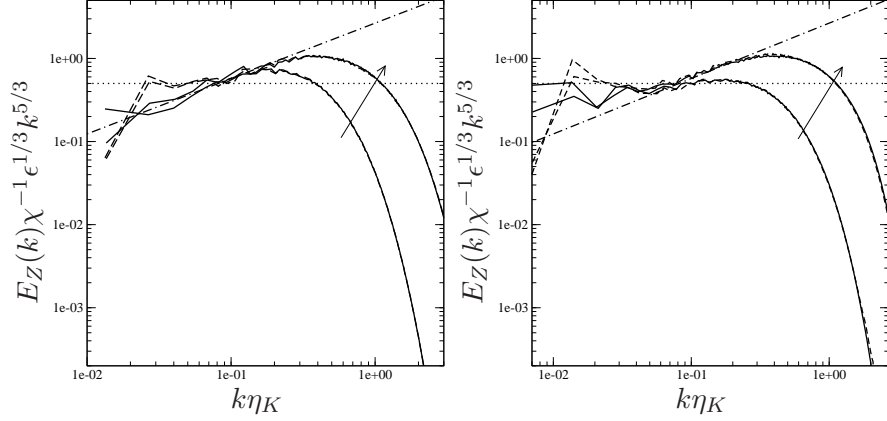


FIG. 5. Scalar variance spectra for two Schmidt number, $Sc = 0.7$ and $Sc = 4$ for $R_\lambda \approx 130$ (left) and $R_\lambda \approx 210$ (right). The spectra are compensated by the scaling proposed by Corrsin-Obukov and the dotted line is for $C_{CO} = 0.5$. The arrow shows the direction of increasing Schmidt numbers. The dashed and solid lines show the spectra for the localized forcing and constant gradient forcing, respectively. The dashed-dotted line corresponds to the k^{-1} scaling under the chosen normalization.

convective range for this moderate Reynolds number, in contrast with previous works⁷, where an imposed mean scalar gradient was used⁸. To better understand the influence of the forcing scheme at large and intermediate scales, additional simulations have been performed with an imposed mean scalar gradient to maintain the scalar variance. Figure 5 compares the scalar variance spectra for two Reynolds number, 130 and 210 and two Schmidt number, 0.7 and 4. The spectra are compensated by using the scaling of the inertial-convective range. As expected the small scales behavior is not influenced by the forcing schemes. But, for moderate Reynolds number, the influence of the forcing schemes clearly appears. The simulations using a mean scalar gradient forcing have no inertial-convective range and the large k^{-1} viscous-convective range seems with result from the forcing. In particular, for $Sc = 0.7$, the scalar spectrum exhibits a viscous-convective range for the mean scalar gradient forcing, in contrast with the results obtained with a low wave numbers forcing and with the theoretical prediction. Note that, when the Reynolds number increases, a inertial-convective range begins to appear for simulations with mean scalar gradient, as shown by the spectra for $R_\lambda = 210$. Future works will be devoted to better understand how this forcing influence on the inertial-convective range.

ACKNOWLEDGMENTS

This work is supported by the Agence Nationale pour la Recherche (ANR) under Contracts No. ANR-2010-JCJC-091601 and ANR-2010-COSI-009. This work was performed using HPC resources from GENCI-IDRIS (Grant 2012-020611). The authors thankfully acknowledge the hospitality of the Center for Turbulence Research, NASA-Ames and Stanford University, where part of this work has been done during the Summer Program 2012. The support of Institut Universitaire de France is gratefully acknowledged by the third author.

-
- ¹ J.-B. Lagaert, G. Balarac, and G.-H. Cottet. Particle method: an efficient tool for direct numerical simulations of a high Schmidt number passive scalar in turbulent flow. *Proceeding of the CTR summer program, Stanford Univ.*, 2012.
 - ² M. Lesieur. *Turbulence in fluids*. Fluid mechanics and its applications. Springer, Dordrecht, 2008.
 - ³ G. K. Batchelor. Small-scale variation of convected quantities like temperature in turbulent fluid part 1. general discussion and the case of small conductivity. *J. Fluid Mech*, 5(01):113–133, 1959.
 - ⁴ S. Corrsin. On the spectrum of isotropic temperature fluctuations in an isotropic turbulence. *J. Appl. Phys.*, 22:469–473, 1951.
 - ⁵ A. M. Obukhov. The structure of the temperature field in a turbulent flow. *Dokl. Akad. Nauk. SSSR*, 39:391, 1949.
 - ⁶ R. Kraichnan. Small-scale structure of a scalar field convected by turbulence. *Phys. Fluids*, 11:945–953, 1968.
 - ⁷ D. A. Donzis, K. R. Sreenivasan, and P. K. Yeung. The batchelor spectrum for mixing of passive scalars in isotropic turbulence. *Flow, Turbulence and Combustion*, 85:549–566, 2010.
 - ⁸ P K Yeung, Shuyi Xu, and K R Sreenivasan. Schmidt number effects on turbulent transport with uniform mean scalar gradient. *Physics of Fluids*, 14(12):4178, 2002.
 - ⁹ G.-H. Cottet, G. Balarac, and M. Coquerelle. Subgrid particle resolution for the turbulent transport of a passive scalar. In *Advances in Turbulence XII, Proceedings of the 12th EUROMECH European Turbulence Conference*, volume 132, pages 779–782, September 2009.
 - ¹⁰ A. Magni and G.H. Cottet. Accurate, non-oscillatory, remeshing schemes for particle methods.

- Journal of Computational Physics*, 231(1):152 – 172, 2012.
- ¹¹ T. Gotoh, S. Hatanaka, and H. Miura. Spectral compact difference hybrid computation of passive scalar in isotropic turbulence. *Journal of Computational Physics*, 231(21):7398–7414, August 2012.
- ¹² K. Alvelius. Random forcing of three-dimensional homogeneous turbulence. *Phys. Fluids*, 11:1880–1889, 1999.
- ¹³ C. da Silva and J. Pereira. Analysis of the gradient-diffusion hypothesis in large-eddy simulations based on transport equations. *Physics of Fluids*, 2007.
- ¹⁴ D.A. Donzis and P.K. Yeung. Resolution effects and scaling in numerical simulations of passive scalar mixing in turbulence. *Physica D*, 239(14):1278–1287, July 2010.
- ¹⁵ K.R. Sreenivasan. The passive scalar spectrum and the Obukhov–Corrsin constant. *Physics of Fluids*, 8:189, 1996.
- ¹⁶ D A Donzis and K R Sreenivasan. The bottleneck effect and the Kolmogorov constant in isotropic turbulence. *Journal of Fluid Mechanics*, 657:171–188, June 2010.
- ¹⁷ S.K. Lee, A. Benaissa, L. Djenidi, P. Lavoie, and R.A. Antonia. Scaling range of velocity and passive scalar spectra in grid turbulence. *Physics of Fluids*, 24:075101, 2012.
- ¹⁸ L. Danaila and R.A. Antonia. Spectrum of a passive scalar in moderate Reynolds number homogeneous isotropic turbulence. *Physics of Fluids*, 21(11):111702, 2009.
- ¹⁹ C. H. Gibson. Fine Structure of Scalar Fields Mixed by Turbulence. II. Spectral Theory. *Physics of Fluids*, 11(11):2316, 1968.
- ²⁰ D.I. Pullin and T.S. Lundgren. Axial motion and scalar transport in stretched spiral vortices. *Physics of Fluids*, 13(9):2553, 2001.
- ²¹ D. Bogucki, H. Luo, and A. J. Domaradzki. Experimental evidence of the Kraichnan scalar spectrum at high reynolds numbers. *J. Phys. Ocean*, 2012. in press.
- ²² D. Bogucki, A. J. Domaradzki, and P. K. Yeung. Direct numerical simulations of passive scalars with $Pr > 1$ advected by turbulent flow. *J. Fluid Mech.*, 343:111–130, 1997.